

Indium-induced reconstructions of the Si(100) surface

A. A. Baski, J. Nogami,* and C. F. Quate

Department of Applied Physics, Stanford University, Stanford, California 94305

(Received 6 November 1990)

The behavior of indium on the Si(100) 2×1 surface has been studied using scanning tunneling microscopy. At temperatures below 150°C, low coverages of In form dimer rows that are oriented perpendicular to the underlying Si dimer rows. As the coverage increases, these rows pack into areas of two-dimensional order, forming the 2×2 reconstruction at 0.5 ML. For substrate temperatures above 150°C, low coverages of In form isolated structures which have two maxima in the empty electronic states and a central maximum in the filled states. As the coverage increases, these In structures arrange into rows oriented parallel to the Si dimer rows with an inter-row spacing of four unit cells. At 0.5 ML, the In structures are spaced three unit cells apart along these rows, thus forming the In (4×3) reconstruction. Evidence for disruption of the substrate Si dimer bonds and Si displacement due to formation of the 4×3 phase is also observed.

The Si(100) surface has been intensively studied by scanning tunneling microscopy as a result of its technological relevance. The 2×1 clean-surface reconstruction involves surface atoms which form rows of dimers. Growth of submonolayer coverages of metals on this surface can be strongly influenced by these Si dimer rows. Here, we present scanning tunneling microscopy (STM) results on the growth of In on the Si(100) surface.

Low-energy electron diffraction (LEED) studies of the In/Si(100) surface indicate two reconstructions between 0.1 and 0.5 monolayers (ML).¹ Below 150°C, In (2×2) coexists with Si (2×1) up to 0.5 ML and In (2×2) occurs at 0.5 ML. Above 150°C, In (4×3) and Si (2×1) coexist up to 0.5 ML and In (4×3) occurs at 0.5 ML. Annealing the In (2×2) structure above 150°C irreversibly transforms the surface to In (4×3) . This study focuses on the evolution of the In (4×3) reconstruction from 0.05 to 0.5 ML. The lower temperature In (2×2) reconstruction, briefly discussed here, is more thoroughly described elsewhere.²

All sample preparation and measurements were performed in an ultra-high vacuum (UHV) system with facilities for both LEED and STM. Two different STM instruments were used during these experiments.³ The Si(100) samples were cut from commercial wafer stock and then cleaned by a UV-ozone process immediately before introduction to vacuum.⁴ In UHV, the wafers were flashed at 1130–1150°C for 2 min held at 1000°C for 10 min, and then slowly cooled. The chamber pressure remained below 2×10^{-9} Torr during flashing. Indium was evaporated from a heated tungsten basket onto substrates at or below 150°C. The deposition rate was calibrated by a quartz-crystal microbalance and the coverage was controlled by timed exposure of the sample to the source. The higher temperature In (4×3) phase was obtained by subsequently annealing the sample to temperatures between 200 and 400°C. All STM imaging was done at room temperature.

A brief description of the lower temperature In (2×2) reconstruction is presented in order to illustrate the bonding behavior observed for deposition temperatures be-

low 150°C. Figures 1(a)–1(c) are three images of the Si(100) surface with nominally 0.05, 0.2, and 0.3 ML In, respectively. As Fig. 1(a) clearly shows, the deposited In appears as bright rows aligned perpendicular to the underlying Si dimer rows. The bright rows are relatively long, indicating anisotropic growth along the In row direction. As the In coverage is gradually increased, the In rows begin to pack into areas of two-dimensional order. Below 0.2 ML coverage, an inter-row spacing of three unit cells ($3a$, where $a=3.84$ Å) frequently appears. When the In coverage is further increased, the In rows become less separated and form regions with a $2a$ inter-row spacing [Fig. 1(b)]. This packing continues until a majority of the surface is covered by In rows at the $2a$ spacing [Fig. 1(c)].

It is also possible to observe in these images a $2a$ periodicity along the In rows. This $2a$ corrugation along the rows, in conjunction with a $2a$ spacing between rows, corresponds to the In (2×2) reconstruction. Comparison of

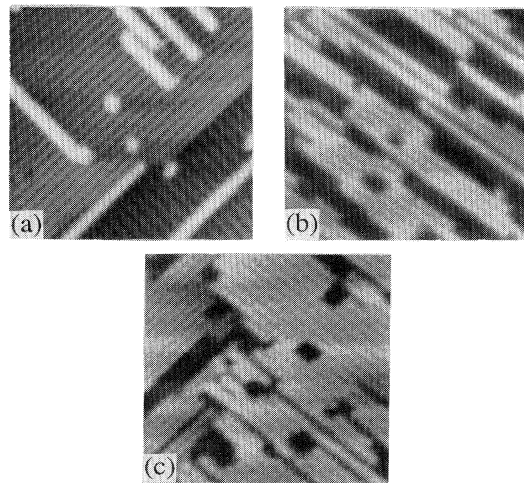


FIG. 1. (a)–(c) Three empty electronic state images (~ 190 Å)² with 0.05, 0.2, and 0.3 ML In deposited at room temperature, respectively.

the nominal In coverage to the observed row density is consistent with a density of one In atom for each Si unit cell along the In rows. Since a $2a$ periodicity is observed along the row, it is reasonable to assume that In atoms are pairing up to form this periodic corrugation. These images are consistent with the formation of In dimers located in the troughs between underlying Si dimer rows. The formation of metal dimers allows the group-III metal adatoms to be threefold coordinated, with each adatom bonded to one metal atom and two substrate Si atoms. Previous work has suggested such a dimer structure for the 2×2 reconstruction formed at 0.5 ML for Al, Ga, and In on Si(100).⁵⁻⁹

In the remainder of this paper, we will focus on the higher temperature In(4×3) reconstruction. Figures 2(a)-2(d) are four images of surfaces with nominally 0.05, 0.2, 0.3, and 0.5 ML In deposited and annealed between 250 and 400 °C, respectively. All the images were taken with a positive tip bias between +1.2 and +2.2 V and, therefore, reveal the filled electronic states of the surface. At the lowest coverage [Fig. 2(a)], the deposited In appears as bright, isolated maxima which are located between Si dimer rows. As the In coverage is gradually increased [Fig. 2(b)], these bright maxima begin to form rows parallel to the Si dimer rows with roughly a $4a$ inter-row separation. Along each of these rows, the In maxima are typically spaced $3a$ or $4a$ apart, with the $3a$ spacing prevalent at higher coverages [Fig. 2(c)]. At 0.5 ML, the surface is well ordered with the In maxima aligned $3a$ apart along rows that are separated by $4a$, corresponding to the In(4×3) reconstruction [Fig. 2(d)]. An example of a phase boundary between two adjacent In(4×3) domains is visible in this image.

Figure 3 is a dual bias image taken tunneling into and out of the same sample area, thus reflecting empty [Fig. 3(a)] and filled electronic states [Fig. 3(b)], respectively. The isolated In structures seen previously in Fig. 2 appear

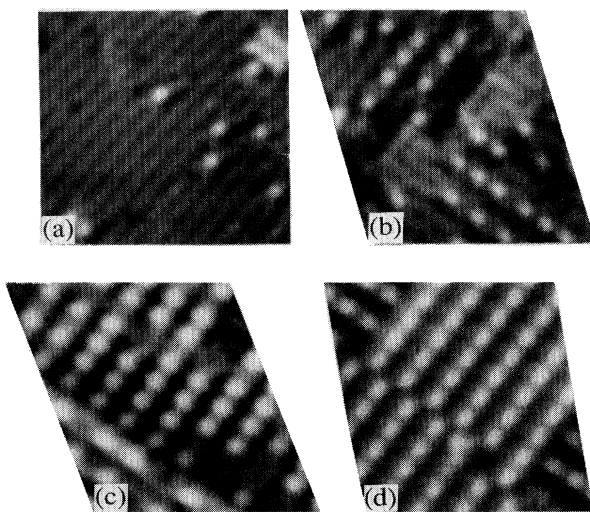


FIG. 2. (a)-(d) Four filled electronic state images ($\sim 105 \text{ \AA}$)² with 0.05, 0.2, 0.3, and 0.5 ML In deposited and annealed, respectively.

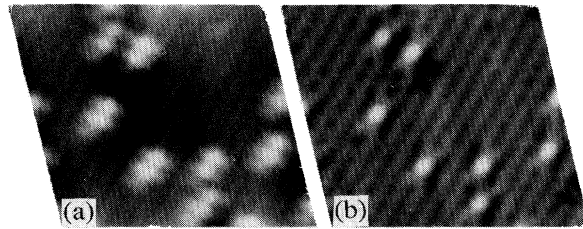


FIG. 3. Dual bias images ($115 \text{ \AA} \times 110 \text{ \AA}$) with 0.05 ML In deposited and annealed. The left- and right-hand side images are taken simultaneously at -1.9-V and $+1.9\text{-V}$ tip bias, thus reflecting (a) empty and (b) filled electronic states of the In subunits.

significantly different in the two biases. Each In subunit consists of two maxima spaced approximately $2a$ apart in the unfilled states and consists of one centrally located maximum in the filled states. In the filled states images [Fig. 3(b)], the Si rows immediately adjacent to each In subunit appear to be significantly disrupted. In addition, the Si dimer rows in the vicinity of an In subunit are usually buckled. These observations suggest that the formation of an In subunit strongly influences the dimer bonding of nearby Si dimers. A similar buckling of dimers also has been observed near alkali-metal atoms adsorbed on Si(100).¹⁰

Figure 4 (upper panel) is a dual bias image of the surface at 0.4 ML coverage. The lower panel shows a cross-sectional trace along the indicated row, intersecting three of the In subunits. The two maxima in empty states (trace a) and one centered maximum in the filled states (trace b) associated with each In subunit are clearly visible in the trace. At this coverage, the In subunits are spaced either $3a$ or $4a$ apart along the row, as marked by the appropriate labels. When the In(4×3) reconstruction

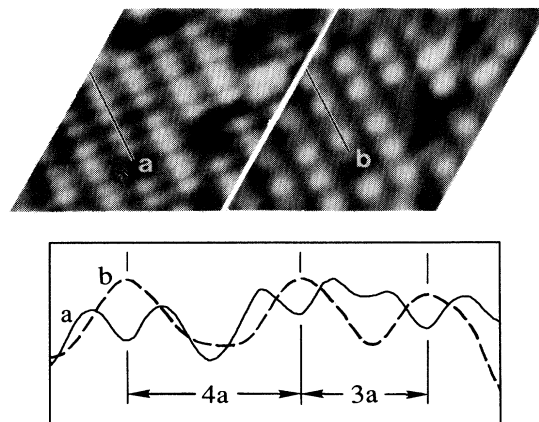


FIG. 4. Upper panel: Dual bias images ($85 \times 100 \text{ \AA}$) with 0.4 ML In deposited and annealed. The left- and right-hand side images are taken at -2.2-V and $+2.2\text{-V}$ tip bias, respectively. Lower panel: A cross sectional trace along a row of In subunits. Each In subunit consists of two maxima spaced approximately $2a$ apart in the empty states (solid line) and one central maximum in the filled states (dashed line); ($a = 3.84 \text{ \AA} = a_0/\sqrt{2}$).

is complete, only the $3a$ spacing exists.

From such dual bias images, it is possible to illustrate the morphology and registration of the In subunits. Figure 5 shows the surface with Si dimers denoted by the small light circles and the empty (filled) electronic states of the In subunits represented by large ovals (black circles). Also shown is the outline of the 4×3 unit cell. The In subunits are located between the Si dimer rows such that the empty and filled states maxima are aligned with the underlying Si dimers. Comparison of the nominal In coverage to the observed density of In subunits indicates that each corresponds to 6 ± 1 In atoms. This assignment is consistent with the result from earlier studies that the $\text{In}(4 \times 3)$ reconstruction is completed at 0.5 ML. Although Fig. 5 does not provide an atomic model of the In subunits, some limitations to a proposed structure are now evident. Any proposed model should incorporate ~ 6 atoms into each In subunit such that the empty and filled electronic states have the separation and registration as given above. In addition, the significant disruption of Si dimer rows near each In subunit, as shown in Fig. 3(b), must be accommodated.

Figures 6(a) and 6(b) are a dual bias image of the surface which shows both In subunits and Si dimer rows. There are two small second layer islands in the lower half of each frame that consist of a few rows which are rotated 90° with respect to the underlying first layer. There is a strong similarity in both the empty and filled electronic states between these rows and the Si dimer rows visible in the upper left hand corner. This similarity supports our assumption that these islands consist of Si atoms. Further evidence that the islands are silicon is the existence of an In subunit with the expected rotated orientation on each island. These small isolated islands are similar to those seen after growth of Si on Si(100).¹¹⁻¹³ Such islands are never observed on the clean surface or on a surface with In deposited below 150°C . They are relatively common, however, on surfaces with In annealed to form areas of the 4×3 phase.

Figure 6(c) is a mosaic showing a surface entirely covered by the $\text{In}(4 \times 3)$ phase at 0.5 ML. A striking aspect of this surface is the existence of numerous terraces that are one step height apart. This terrace structure is unrelated to the surface vicinality because it is present in regions with no net tilt as shown. Since the upper terraces

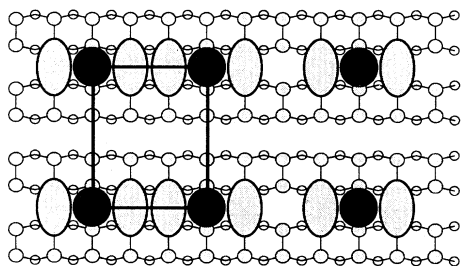


FIG. 5. An illustration of the In subunit configuration where Si dimers are denoted by the small light circles and the empty (filled) electronic states of the In subunits are represented by large ovals (black circles).

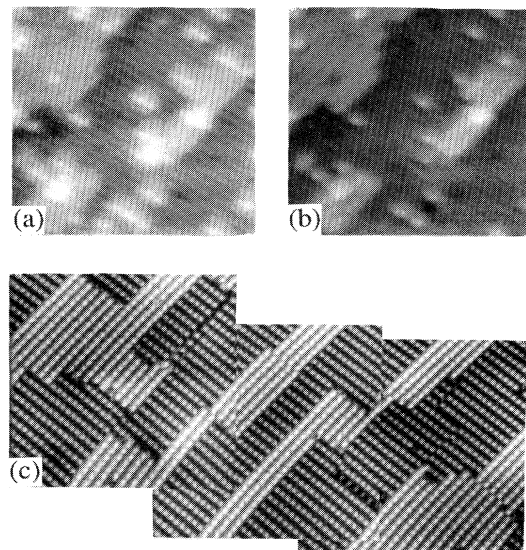


FIG. 6. (a) and (b) Dual bias images $(175 \text{ \AA})^2$ with 0.05 ML In deposited and annealed, are taken at -1.9-V and $+1.9\text{-V}$ tip bias and 1.3-nA tunneling current, respectively. Small islands exist which may be caused by displaced silicon. (c) A mosaic of three $(350 \text{ \AA})^2$ images with 0.5 ML In deposited and annealed. Each image was taken at 1.5-V tip bias and 3.3-nA tunneling current. Second layer islands covered with rotated domains of $\text{In}(4 \times 3)$ appear on the surface.

cover $\sim 40\%$ of the surface at 0.5 ML In coverage, it is also unlikely that they are due to second layer In growth. The $\text{In}(4 \times 3)$ structure on the upper terraces is rotated 90° with respect to that on the lower terraces, just as observed for a Si step. The step height difference and rotation of surface structure between the first and second layers suggest that the upper terraces are Si islands terminated by $\text{In}(4 \times 3)$. This result, as well as the Si islands observed at low coverage, suggest that the formation of the $\text{In}(4 \times 3)$ phase is accompanied by displacement of Si surface atoms. These displaced Si atoms form second layer islands upon which $\text{In}(4 \times 3)$ grows.

Antiphase boundaries are visible in the $\text{In}(4 \times 3)$ structure for both the first and second layers. At these boundaries, the adjacent $\text{In}(4 \times 3)$ domains can be shifted by one, two, or three unit cells along the $4x$ direction. When the first layer $\text{In}(4 \times 3)$ domains on either side of a second layer island are compared, a majority of the islands are found to lie along phase boundaries. A random-phase relationship between two such first layer domains would result in a phase slip 75% of the time. Our data shows a slightly higher frequency, but the difference may not be statistically significant. This relationship between phase boundaries and second layer islands suggests two possible behaviors. One possibility is that the islands merely act as a dividing line between first layer domains so that the phase relationship between two domains on either side of an island is random. The other is that the presence of a phase boundary in the first layer actually plays a role in preferentially nucleating second layer growth, as seen for Si growth on both Si(100) and

Si(111).^{11,14} The fact that phase boundaries are visible in the first layer without areas of second layer growth suggests that preferential nucleation does not play as large a role as in Si homoepitaxy.

Since adjacent In(4×3) domains can be shifted by an odd number of unit cells along the 4× direction, the 2×1 Si dimerization must be broken under the 4×3 phase. In the case of small islands of 4×3, a specific registration is maintained with respect to the surrounding Si dimerization, possibly reflecting the influence of the dimerization on nucleation at low coverages. This phase relationship with the 2×1 no longer exists at higher coverages when a majority of the surface is covered by 4×3. Unlike the In(4×3) phase, the In(2×2) structure involves In dimer rows that always remain in registration with the substrate, suggesting that Si dimerization may not be removed underneath the adsorbed In. Calculations for the Al/Si(100) 2×2 structure have shown that it is energetically favorable for the Si dimerization to be removed, but the energy gain is relatively small.¹⁵

In conclusion, we have described both the In(2×2) and In(4×3) reconstructions which result from deposition of up to 0.5 ML of In onto the Si(100) surface. At temperatures below 150°C, In lines up with a 2*a* periodicity in

rows perpendicular to the underlying Si dimer rows. It is the packing of these rows into arrays with a 2*a* inter-row spacing that forms the In(2×2) phase. The registration and density of the In features in the STM images are consistent with In bonding as dimers in the troughs between the Si dimer rows. At temperatures above 150°C, In forms subunits which contain approximately six atoms. These subunits consist of two maxima separated by roughly two unit cells in the empty electronic states and a central maximum in the filled states. As the coverage increases, these In subunits arrange into rows oriented parallel to the Si dimer rows with a 4*a* inter-row spacing. At 0.5 ML, the In subunits become spaced 3*a* apart along these rows and, thus, form the In(4×3) reconstruction. The presence of second layer islands on the surface indicates that Si displacement occurs during the formation of this phase. In addition, there is evidence that the In(4×3) phase "unzips" the underlying Si dimer rows, unlike the lower temperature In(2×2) phase.

This research was supported by the Office of Naval Research. One of the authors (A.A.B.) acknowledges support from AT&T.

*Present address: Department of Physics, University of Wisconsin-Milwaukee, Milwaukee, WI 53201.

¹J. Knall, J.-E. Sundgren, G. V. Hansson, and J. E. Greene, *Surf. Sci.* **166**, 512 (1986).

²A. A. Baski, J. Nogami, and C. F. Quate, *J. Vac. Sci. Technol. A* (to be published).

³Sang-il Park and C. F. Quate, *Rev. Sci. Instrum.* **58**, 2010 (1987). Commercial STM provided by Park Scientific Instruments, Inc., Mountain View, CA.

⁴M. Tabe, *Appl. Phys. Lett.* **45**, 1073 (1984).

⁵T. Ide, T. Nishimori, and T. Ichinokawa, *Surf. Sci.* **209**, 335 (1989).

⁶B. Bourguignon, K. L. Carleton, and S. R. Leone, *Surf. Sci.* **204**, 455 (1988).

⁷D. H. Rich, A. Samsavar, T. Miller, H. F. Lin, and T.-C. Chiang, *Phys. Rev. Lett.* **58**, 579 (1987).

⁸J. Nogami, Sang-il Park, and C. F. Quate, *Appl. Phys. Lett.* **53**,

2086 (1988).

⁹A. A. Baski, J. Nogami, and C. F. Quate, *J. Vac. Sci. Technol. A* **8**, 245 (1990).

¹⁰T. Hashizume, Y. Hasegawa, I. Kamiya, T. Ide, I. Sumita, S. Hyodo, T. Sakurai, H. Tochiyama, M. Kubota, and Y. Murata, *J. Vac. Sci. Technol. A* **8**, 233 (1990).

¹¹R. J. Hamers, U. K. Köhler, and J. E. Demuth, *J. Vac. Sci. Technol. A* **8**, 195 (1990).

¹²Y.-W. Mo, R. Kariotis, B. S. Swartzentruber, M. B. Webb, and M. G. Lagally, *J. Vac. Sci. Technol. A* **8**, 201 (1990).

¹³A. J. Hoeven, D. Dijkkamp, E. J. van Loenen, J. M. Lenssinck, and J. Dieleman, *J. Vac. Sci. Technol. A* **8**, 207 (1990).

¹⁴U. Köhler, J. E. Demuth, and R. J. Hamers, *J. Vac. Sci. Technol. A* **7**, 2860 (1989).

¹⁵Inder P. Batra, *Phys. Rev. Lett.* **63**, 1704 (1989).

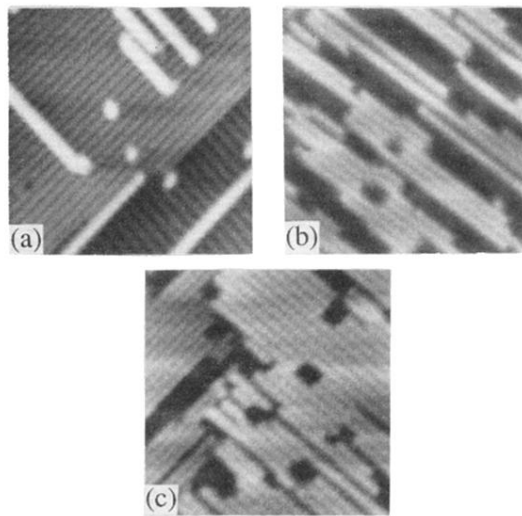


FIG. 1. (a)-(c) Three empty electronic state images ($\sim 190 \text{ \AA}$)² with 0.05, 0.2, and 0.3 ML In deposited at room temperature, respectively.

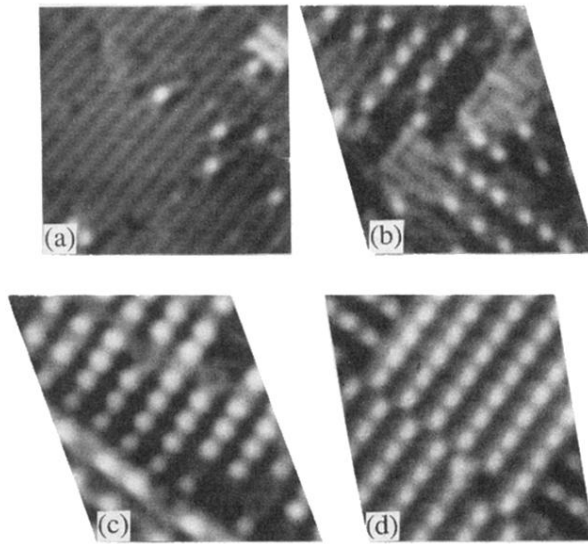


FIG. 2. (a)-(d) Four filled electronic state images ($\sim 105 \text{ \AA}^2$) with 0.05, 0.2, 0.3, and 0.5 ML In deposited and annealed, respectively.

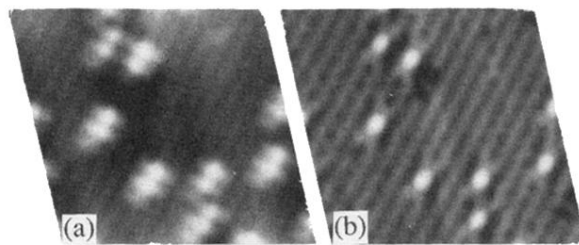


FIG. 3. Dual bias images ($115 \text{ \AA} \times 110 \text{ \AA}$) with 0.05 ML In deposited and annealed. The left- and right-hand side images are taken simultaneously at -1.9-V and $+1.9\text{-V}$ tip bias, thus reflecting (a) empty and (b) filled electronic states of the In subunits.

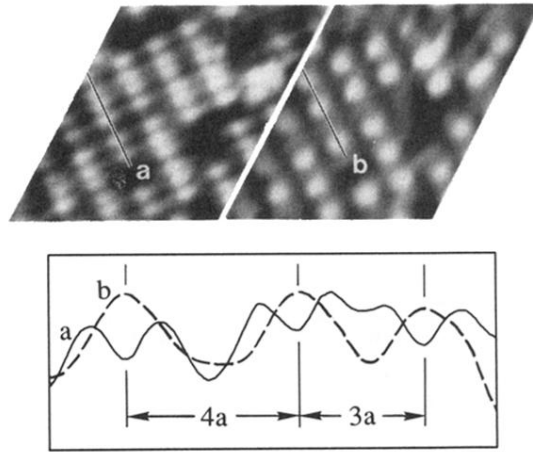


FIG. 4. Upper panel: Dual bias images ($85 \times 100 \text{ \AA}$) with 0.4 ML In deposited and annealed. The left- and right-hand side images are taken at -2.2-V and $+2.2\text{-V}$ tip bias, respectively. Lower panel: A cross sectional trace along a row of In subunits. Each In subunit consists of two maxima spaced approximately $2a$ apart in the empty states (solid line) and one central maximum in the filled states (dashed line); ($a = 3.84 \text{ \AA} = a_0/\sqrt{2}$).

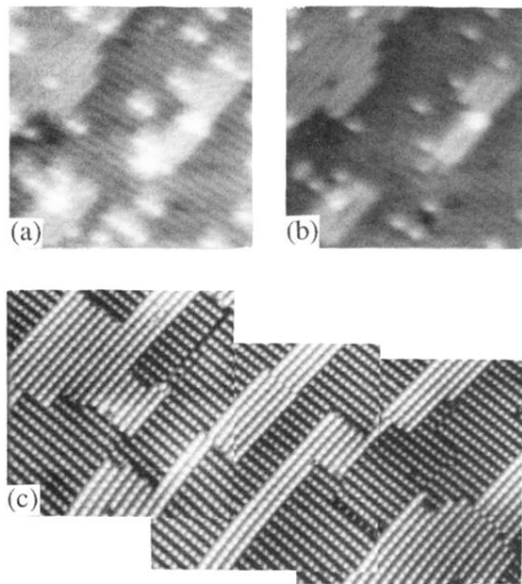


FIG. 6. (a) and (b) Dual bias images $(175 \text{ \AA})^2$ with 0.05 ML In deposited and annealed, are taken at -1.9-V and $+1.9\text{-V}$ tip bias and 1.3-nA tunneling current, respectively. Small islands exist which may be caused by displaced silicon. (c) A mosaic of three $(350 \text{ \AA})^2$ images with 0.5 ML In deposited and annealed. Each image was taken at 1.5-V tip bias and 3.3-nA tunneling current. Second layer islands covered with rotated domains of $\text{In}(4 \times 3)$ appear on the surface.